

# Structures and Conformations of Trifluoromethyl Fluoroformate and Perfluorodimethyl Carbonate

Angelika Hermann,<sup>†</sup> Frank Trautner,<sup>†</sup> Khodayar Gholivand,<sup>‡,§</sup> Stefan von Ahsen,<sup>‡</sup>  
Eduardo L. Varetti,<sup>‡,||</sup> Carlos O. Della Vedova,<sup>‡,⊥</sup> Helge Willner,<sup>\*,‡</sup> and Heinz Oberhammer<sup>\*,†</sup>

Institut für Physikalische und Theoretische Chemie, Universität Tübingen, D-72076 Tübingen, Germany, Anorganische Chemie, FB 6, Universität GH Duisburg, D-47048 Duisburg, Germany, and CEQUINOR (CONICET), Departamento de Química, Facultad de Ciencias Exactas, Universidad Nacional de La Plata, 47 esq. 115, 1900 La Plata, Argentina

Received January 17, 2001

The conformational properties and geometric structures of trifluoromethyl fluoroformate, CF<sub>3</sub>OC(O)F (**1**), and perfluorodimethyl carbonate, (CF<sub>3</sub>O)<sub>2</sub>CO (**2**), have been studied by matrix IR spectroscopy, gas electron diffraction (GED), and quantum chemical calculations (MP2 and B3LYP with 6-311G\* basis sets). In both compounds the synperiplanar orientation of the O–CF<sub>3</sub> groups relative to the C=O double bond is preferred. If heated Ar/1 and Ar/2 mixtures are deposited as a matrix at 14 K, new bands appear in the matrix IR spectra which are assigned to the anti form of **1** and to the syn/anti form of **2**. At room temperature the contribution of the anti rotamer of **1** is 4% ( $\Delta H^\circ = H^\circ(\text{anti}) - H^\circ(\text{syn}) = 1.97(5)$  kcal/mol), and the contribution of the syn/anti conformer of **2** is estimated to be less than 1%. These high-energy conformers are not observed in the GED experiment. The quantum chemical calculations reproduce the structural and conformational properties of both compounds satisfactorily.

## Introduction

Conjugation between the p-shaped oxygen lone pair and a  $\pi$  bond plays an important role in structural chemistry. Well-known examples are methyl formate, CH<sub>3</sub>OC(O)H,<sup>1–3</sup> and methyl vinyl ether, CH<sub>3</sub>OC(H)=CH<sub>2</sub>.<sup>4–6</sup> In both compounds conjugation results in sterically unfavorable synperiplanar orientation of the O–C(sp<sup>3</sup>) bond relative to the double bond. In the former compound orbital interaction occurs between the lone pair and the C=O bond ( $n_\pi(\text{O}) \rightarrow \pi^*(\text{C}=\text{O})$ ) and in the latter compound between the lone pair and the C=C bond ( $n_\pi(\text{O}) \rightarrow \pi^*(\text{C}=\text{C})$ ). Conjugation between oxygen lone pairs and the C=O bond also leads to a planar syn/syn structure of dimethyl carbonate, with both O–C(sp<sup>3</sup>) bonds syn to the C=O bond.<sup>7</sup>

Perfluorination of methyl vinyl ether leads to a strong conformational change.<sup>8</sup> In CF<sub>3</sub>OC(F)=CF<sub>2</sub> the O–C(sp<sup>3</sup>) bond is nearly perpendicular to the plane of the vinyl group

( $\phi(\text{C}=\text{C}-\text{O}-\text{C}) = 104(2)^\circ$ ), and no conjugation is present in this compound. In view of this strong effect of fluorination in methyl vinyl ether, it appeared interesting to investigate this effect in methyl formate and dimethyl carbonate. The structures and conformational properties of trifluoromethyl fluoroformate, CF<sub>3</sub>OC(O)F (**1**), and perfluorodimethyl carbonate, (CF<sub>3</sub>O)<sub>2</sub>CO (**2**), were studied using matrix IR spectroscopy, gas electron diffraction (GED), and quantum chemical calculations.

Compounds **1** and **2** had been prepared for the first time by dimerization and trimerization of carbonyl fluoride, respectively.<sup>9</sup> Subsequently they were synthesized more efficiently by photolysis of CO/CF<sub>3</sub>OF<sup>10</sup> or CO/CF<sub>3</sub>OOCF<sub>3</sub><sup>11</sup> mixtures. Vibrational spectra of **1** were interpreted on the basis of a single conformer with a synperiplanar structure and C<sub>s</sub> symmetry.<sup>12,13</sup> The IR spectrum of **2** was assigned for a syn/syn conformation with C<sub>2v</sub> symmetry.<sup>14,15</sup>

## Experimental Section

According to the literature procedure the synthesis of **1** and **2** was accomplished by photolysis of a mixture of CF<sub>3</sub>OF/CO<sup>10</sup> and CF<sub>3</sub>OOCF<sub>3</sub>/CO,<sup>11</sup> respectively. The products were purified by repeated trap-to-trap distillation in vacuo, and the final purity (> 98%) was checked by IR<sup>13,14</sup> and NMR<sup>16</sup> spectroscopy. The pure compounds were stored

\* To whom correspondence should be addressed. (H.O.) E-mail: heinz.oberhammer@uni-tuebingen.de. Fax: +49-7071-295490. (H.W.) E-mail: willner@uni-duisburg.de. Fax: +49-203-379-2231.

<sup>†</sup> Universität Tübingen.

<sup>‡</sup> Universität GH Duisburg.

<sup>§</sup> Permanent address: Tarbiat Modarres University, P.O. Box 14155-4838, Teheran, Iran.

<sup>||</sup> Permanent address: CEQUINOR (CONICET-UNLP), Universidad Nacional de La Plata.

<sup>⊥</sup> Permanent address: CEQUINOR (CONICET-UNLP) and Laboratorio de Servicios a la Industria y al Sistema Científico (UNLP-CIC-CONICET), Universidad Nacional de La Plata.

(1) Curl, R. F. *J. Chem. Phys.* **1959**, *30*, 1529.

(2) Shen, Q. *Acta Chem. Scand.* **1977**, *A31*, 795.

(3) Cradock, S.; Rankin, D. W. H. *J. Mol. Struct.* **1980**, *69*, 145.

(4) Owen, N. L.; Seip, H. M. *Chem. Phys. Lett.* **1970**, *5*, 162.

(5) Samdal, S.; Seip, H. M. *J. Mol. Struct.* **1975**, *28*, 193.

(6) Fujitake, M.; Hayashi, M. *J. Mol. Struct.* **1985**, *127*, 21.

(7) Mijlhoff, F. C. *J. Mol. Struct.* **1977**, *36*, 334.

(8) Leibold, C.; Reinemann, S.; Minkwitz, R.; Resnik, P. R.; Oberhammer, H. *J. Org. Chem.* **1997**, *62*, 6160.

(9) Anderson, B. C.; Morlock, G. R. U.S. Patent 3,226,418, 1965; *Chem. Abstr.* **1966**, *64*, 9598.

(10) Aymonino, P. J. *Chem. Commun.* **1965**, 241.

(11) Varetti, E. L.; Aymonino, P. J. *Chem. Commun.* **1967**, 680. Varetti, E. L.; Aymonino, P. J. *An. Asoc. Quim. Argent.* **1967**, *55*, 153.

(12) Varetti, E. L.; Aymonino, P. J. *J. Mol. Struct.* **1967–1968**, *1*, 39.

(13) Cutin, E. H.; Della Vedova, C. O.; Aymonino, P. J. *An. Asoc. Quim. Argent.* **1985**, *73*, 171.

(14) Varetti, E. L.; Aymonino, P. J. *J. Mol. Struct.* **1971**, *7*, 155.

(15) Cutin, E. H.; Della Vedova, C. O.; Varetti, E. L.; Aymonino, P. J. *An. Asoc. Quim. Argent.* **1984**, *72*, 523.

(16) Argüello, G. A.; Willner, H.; Malanca, F. E. *Inorg. Chem.* **2000**, *39*, 1195.

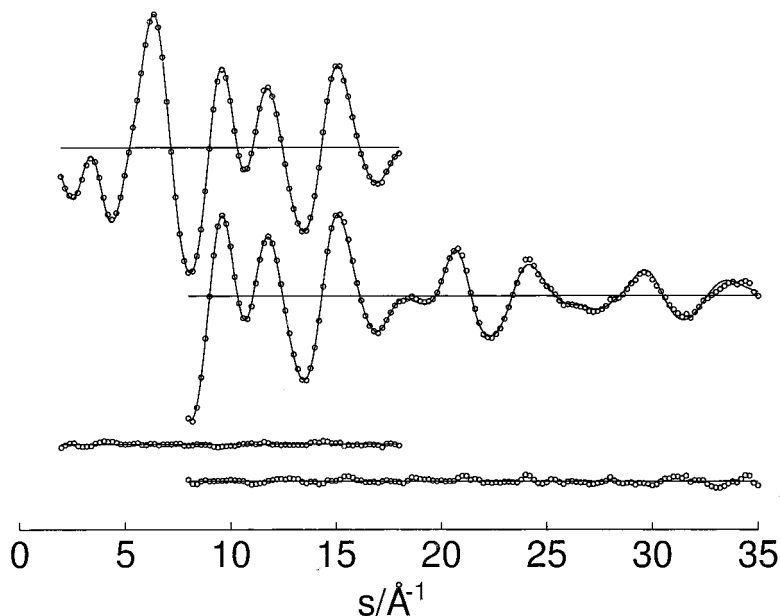


**Figure 1.**  $\text{CF}_3\text{OC}(\text{O})\text{F}$ : experimental (dots) and calculated (full line) molecular intensities for long (top) and short (bottom) nozzle-to-plate distances and residuals.

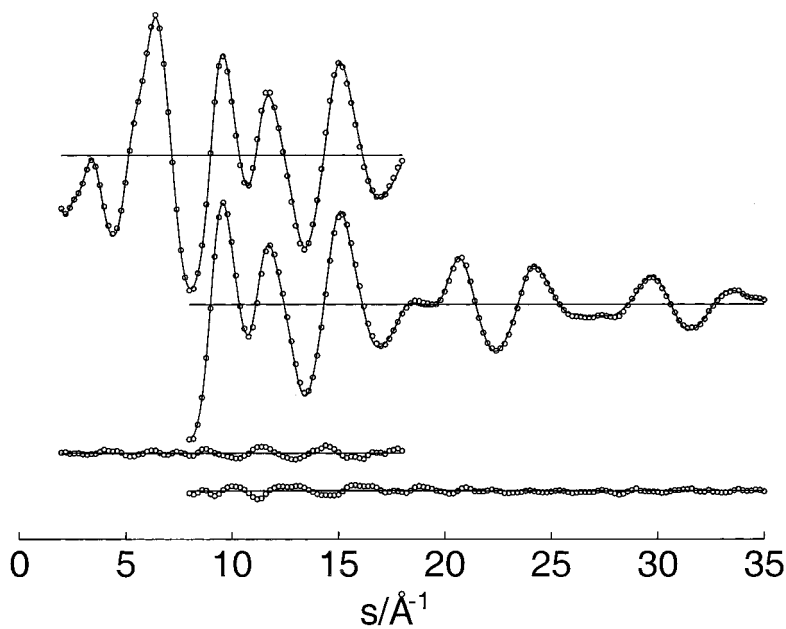


**Figure 2.**  $(\text{CF}_3\text{O})_2\text{CO}$ : experimental (dots) and calculated (full line) molecular intensities for long (top) and short (bottom) nozzle-to-plate distances and residuals.

in flame-sealed glass ampules in a refrigerator. The ampules were opened and resealed by use of an ampule key.<sup>17</sup>

Mixtures of **1** or **2** with Ar (1:500 or 1:2000) were deposited at 14 K on an aluminum-plated copper mirror in a He-cooled cryostat.<sup>18</sup> The mixture was passed through the hot tip of a quartz nozzle immediately before deposition, at temperatures between 25 and 500 °C. IR spectra were recorded with an apodized resolution of 1  $\text{cm}^{-1}$  in the range 4000–400  $\text{cm}^{-1}$  using the reflection technique with a Bruker IFS 66v spectrometer.

Electron diffraction intensities for both compounds were recorded with a Gasdiffraktograph KD-G2<sup>19</sup> at 25 and 50 cm nozzle-to-plate distances and with an accelerating voltage of ca. 60 kV. The sample reservoirs were cooled to –80 °C (**1**) or –55 °C (**2**), and the inlet

system with the nozzle was at room temperature. The photographic plates were analyzed with the usual procedures,<sup>20</sup> and averaged intensities in the ranges 2–18 and 18–35  $\text{Å}^{-1}$  in intervals of  $\Delta s = 0.2 \text{ Å}^{-1}$  are shown in Figures 1 and 2 ( $s = (4\pi/\lambda) \sin \theta/2$ ,  $\lambda$  electron wavelength,  $\theta$  scattering angle).

### Quantum Chemical Calculations

The geometries of the syn and anti conformers of **1** and of the syn/syn and syn/anti conformers of **2** were fully optimized with MP2 and B3LYP approximations, using 6-311G\* basis sets. Both methods predict the syn conformation of **1** to be lower in energy relative to the anti form by 2.89 (MP2) and 2.15 (B3LYP) kcal/mol. For **2** the syn/syn form is predicted to be preferred by 3.22 (MP2) and 2.51 kcal/mol (B3LYP) relative to the syn/anti conformation. The potential functions for internal rotation around the  $\text{C}(\text{sp}^2)\text{—O}$  bond in methyl formate and

(17) Gombler, W.; Willner, H. *J. Phys. E: Sci. Instrum.* **1987**, *20*, 1286.

(18) Argüello, G. A.; Grothe, H.; Kronberg, M.; Willner, H.; Mack, H.-G. *J. Phys. Chem.* **1995**, *99*, 17525.

(19) Oberhammer, H. *Molecular Structure by Diffraction Methods*; The Chemical Society: London, 1976; Vol. 4, p 24.

(20) Oberhammer, H.; Gombler, W.; Willner, H. *J. Mol. Struct.* **1981**, *70*, 273.

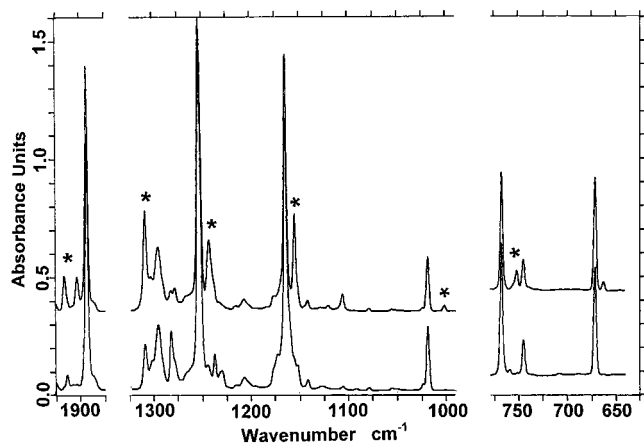


**Figure 3.** IR spectra of CF<sub>3</sub>OC(O)F isolated in an Ar matrix (1:500) at 14 K. Lower trace: spray on nozzle held at 25 °C. Upper trace: spray on nozzle held at 400 °C. The asterisks indicate bands of the anti rotamer.

in **1** were derived with the B3LYP method, performing geometry optimizations for fixed dihedral angles  $\Phi(\text{O}=\text{C}-\text{O}-\text{C})$ . Vibrational frequencies were calculated with the B3LYP/6-31G\* method and are compared to experimental values in the respective tables. Vibrational amplitudes for the low-energy conformers of both compounds were derived from theoretical (B3LYP/6-31G\*) Cartesian force constants. All quantum chemical calculations were performed with the GAUSSIAN98 program suite,<sup>21</sup> and vibrational amplitudes were derived with the program ASYM40.<sup>22</sup>

### Matrix Infrared Spectra

IR spectra of **1** isolated in an Ar matrix are depicted in Figure 3. When the Ar/**1** mixture is passed through the heated deposition nozzle, a new set of bands appear near the ones already present in the IR spectrum, obtained with the deposition nozzle at room temperature. Those new bands are assigned to the higher energy conformer of **1** and are listed in Table 1. The complete sets of calculated (B3LYP/6-31G\*) IR band positions and IR intensities of the syn and anti rotamers are given in Table S1 in the Supporting Information. The calculated wavenumbers for the syn isomer agree rather well with the gas-phase values. When the calculated syn–anti band shifts are compared with the measured ones (Table 1), the agreement is overall good, indicating that the proposed anti rotamer is the most likely species to explain the new bands. One calculated shift of  $-23\text{ cm}^{-1}$  associated with the (calculated)  $1289\text{ cm}^{-1}$  band is not obvious in the spectra. The only feature which could be associated with the corresponding anti rotamer band is the shoulder located at ca.  $1237\text{ cm}^{-1}$ . However, this shoulder coincides with a band of F<sub>2</sub>CO, which is present in small quantities in our matrix spectra. The apparently single matrix band at  $1254\text{ cm}^{-1}$  results from the overlap of two different bands, as predicted by the calculations ( $1290$  and  $1289\text{ cm}^{-1}$ ).

**Table 1.** Observed and Calculated Infrared Wavenumbers for the Syn and Anti Rotamers of CF<sub>3</sub>OC(C)F

gas phase <sup>a</sup>	syn rotamer		anti rotamer		$\Delta s/a^c$ (calcd)	$\Delta s/a^c$ (exptl)
	Ar matrix	calcd <sup>b</sup>	Ar matrix	calcd <sup>b</sup>		
1900	1893	1956	1916	1980	24	23
1300	1295	1331	1308	1339	8	13
1261	1254	1290	1243	1278	-12	-10
1261	1254	1289	1237 sh	1266	-23	ca. -17
1176	1164	1187	1155	1178	-9	-9
1020	1018	1036	1001	1014	-22	-17
891	882	889	853	856	-33	-29
767	767	759	751	746	-13	-16
745	745	738	740 sh	735	-3	ca. -5
673	671	665	671	665	0	0
616	619	608	616	605	-3	-3
562	561	549	553	537	-12	-8

<sup>a</sup> Gas-phase values are taken from refs 12 and 13. <sup>b</sup> B3LYP/6-31G\*. Wavenumbers of the fundamentals are ordered according to the equivalent modes of vibration in both rotamers. <sup>c</sup> Wavenumber differences between the syn and anti conformers.

All bands which grow in intensity upon nozzle heating are already present in the matrix spectrum of a sample deposited with the nozzle held at room temperature. That means that the high-energy anti conformer is in equilibrium with the syn conformer in the gas phase at room temperature. Annealing of the matrix samples to 35 K for a few minutes resulted in the appearance of bands at  $1887$ ,  $1262$  (sh),  $1244$  (sh),  $1177$ , and  $1025\text{ cm}^{-1}$  due to aggregates, while the new rotamer bands were not affected. This behavior differs notably from the results obtained in similar experiments made with matrix-isolated oxalyl fluoride, in which the bands due to the less stable rotamer disappeared on annealing.<sup>23</sup> The height of the barrier to internal rotation in **1**, which is predicted to be  $7.5\text{ kcal/mol}$  (B3LYP), explains why the annealing procedure does not affect the relative intensities of the rotamer bands.

The area ratios of the related pairs of bands belonging to both rotamers were determined and plotted on a logarithmic scale as a function of the inverse of the absolute temperature. Such a van't Hoff plot, represented in Figure 4 for one of the band pairs ( $1164/1155\text{ cm}^{-1}$ ), yielded an enthalpy difference  $\Delta H^\circ = 1.97(5)\text{ kcal/mol}$  (the values obtained for five other pairs of bands, at  $1893/1916$ ,  $1295/1308$ ,  $1164/1155$ ,  $1018/1001$ , and  $767/751\text{ cm}^{-1}$ , do not differ by more than  $0.01\text{ kcal/mol}$  from the given value). The B3LYP method ( $\Delta H^\circ = 2.02\text{ kcal/mol}$ ) reproduces exactly this experimental value, whereas the MP2 approximation ( $\Delta H^\circ = 2.76\text{ kcal/mol}$ ) predicts a higher value. The corrections between  $\Delta E$  and  $\Delta H^\circ$  were derived with the B3LYP/6-312G\* method. From the experimental enthalpy difference a contribution of 4% of the anti rotamer is obtained at room temperature.

**2** was studied in a similar way by IR matrix spectroscopy. At higher nozzle temperatures new bands appeared in the IR spectra due to a higher energy conformer. With the nozzle held at room temperature, however, no bands of this high-energy conformer could be detected in the IR spectrum. The band positions of both species are listed in Table 2, and they agree reasonably well with the calculated (B3LYP/6-31G\*) frequencies of the syn/syn and syn/anti rotamers of **2**. All calculated IR band positions and IR intensities for the fundamentals of both rotamers are given in Table S2 in the Supporting Information. Since no syn/anti rotamer could be detected at room

(21) Frisch, M. J.; Trucks, G. W.; Schlegel, H. B.; Scuseria, G. E.; Robb, M. A.; Cheeseman, J. R.; Zakrzewski, V. G.; Montgomery, J. A.; Stratman, R. E.; Burant, J. C.; Dapprich, S.; Millam, J. M.; Daniels, A. D.; Kudin, K. N.; Strain, M. C.; Farkas, O.; Tomasi, J.; Barone, V.; Cossi, M.; Cammi, R.; Mennucci, B.; Pomelli, C.; Adamo, C.; Clifford, S.; Ochterski, J.; Petersson, G. A.; Ayala, P. Y.; Cui, Q.; Morokuma, K.; Malick, D. K.; Rabuck, A. D.; Raghavachari, K.; Foresman, J. B.; Cioslowski, J.; Ortiz, J. V.; Stefanov, B. B.; Liu, G.; Liashenko, A.; Piskorz, P.; Komaromi, I.; Gomperts, R.; Martin, R. L.; Fox, D. J.; Keith, T.; Al-Laham, M. A.; Peng, C. Y.; Nanayakkara, A.; Gonzalez, C.; Challacombe, M.; Gill, P. M. W.; Johnson, B.; Chen, W.; Wong, M. W.; Andres, J. L.; Gonzalez, C.; Head-Gordon, M.; Replogle, P. M.; Pople, J. A. *GAUSSIAN 98*, Revision A.6; Gaussian, Inc.: Pittsburgh, PA, 1998.

(22) Hedberg, L.; Mills, I. M. *J. Mol. Spectrosc.* **1993**, *160*, 117.

(23) Sander, S.; Willner, H.; Khriachtchev, L.; Pettersson, M.; Räsänen, M.; Varetto, E. L. *J. Mol. Spectrosc.* **2000**, *203*, 145.

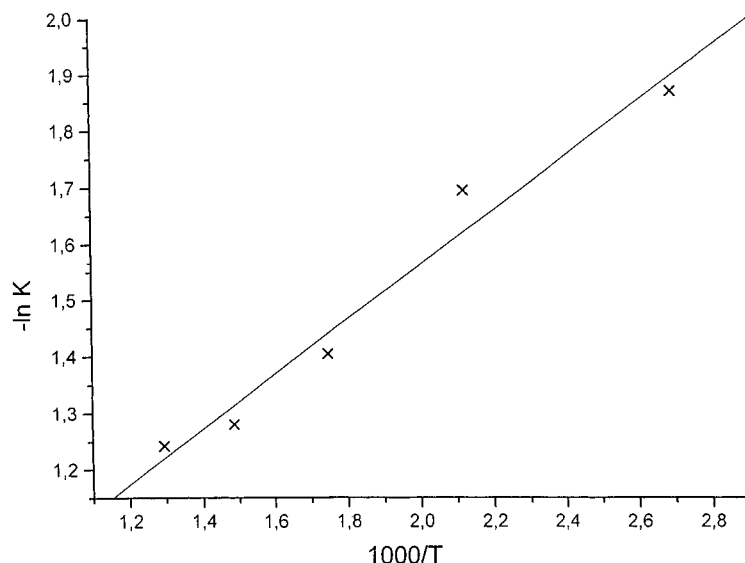


**Figure 4.** van't Hoff plot using the integrated band areas of the IR matrix bands at 1164/1155  $\text{cm}^{-1}$  obtained after the rotamer equilibrium of the syn and anti forms of  $\text{CF}_3\text{OC}(\text{O})\text{F}$  was quenched from different nozzle temperatures.

**Table 2.** Observed and Calculated Infrared Wavenumbers for the Syn/Syn and Syn/Anti Rotamers of  $(\text{CF}_3\text{O})_2\text{CO}$

syn/syn rotamer			syn/anti rotamer		$\Delta s/a^b$ (calcd)	$\Delta s/a^b$ (exptl)
gas phase	Ar matrix	calcd <sup>a</sup>	Ar matrix	calcd <sup>a</sup>		
1865	1858	1912	1870	1928	16	12
		1292	1296	1303	7	11
1292	1289	1287	1284	1280	-7	-5
1261	1258	1253		1248	-10	
		1253		1245	-13	
		1224	1220	1204	-27	-20
1118	1106	1095	1116	1103	8	10
1057	1055	1062	1039	1041	-21	-16
911	918	912	918	911	-1	0
889	888	868	888	868	0	0
769	767	771	752	756	-15	-15
740	734	731	730	726	-5	-4
617	616	612	627	620	8	11

<sup>a</sup> B3LYP/6-31G\*. <sup>b</sup> Wavenumber differences between the syn/syn and syn/anti and anti conformers.

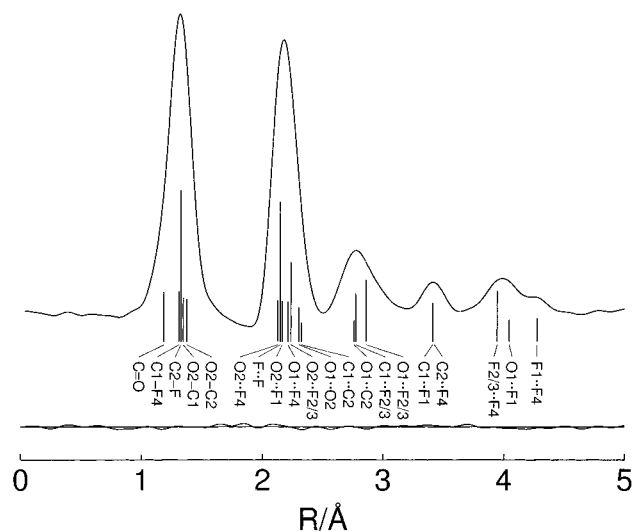


**Figure 5.**  $\text{CF}_3\text{OC}(\text{O})\text{F}$ : experimental radial distribution function and difference curve.

temperature, we conclude that less than 1% of the syn/anti rotamer is present. This is in close agreement with the quantum

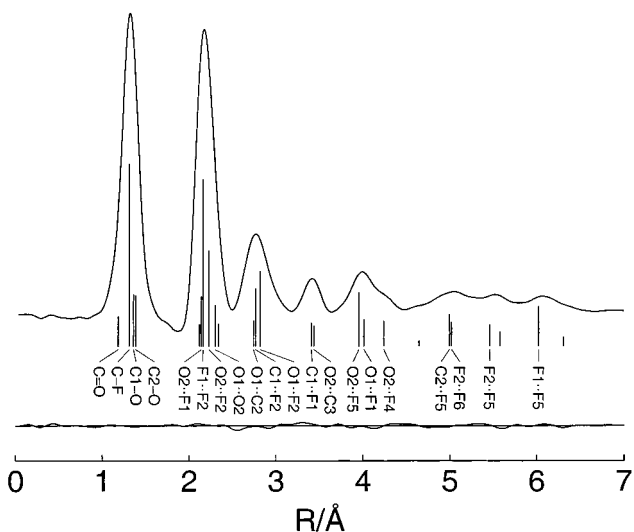


**Figure 6.**  $(\text{CF}_3\text{O})_2\text{CO}$ : experimental radial distribution function and difference curve.

chemical calculations which predict energy differences of 3.22 (MP2) and 2.51 (B3LYP) kcal/mol.

### Structure Analyses

Radial distribution functions (RDFs) were derived by Fourier transformation of the molecular intensities, applying an artificial damping function,  $\exp(-\gamma s^2)$  with  $\gamma = 0.0019 \text{ \AA}^2$ . The RDF for **1** (Figure 5) is reproduced satisfactorily with a synperiplanar conformation and that of **2** (Figure 6) only with a syn/syn structure. The geometric parameters were refined by least-squares fitting of the molecular intensities. The following assumptions were made in these refinements: (i) The structures of **1** and **2** were constrained to  $C_s$  and  $C_{2v}$  symmetry, respectively. (ii) Local  $C_{3v}$  symmetry was assumed for the  $\text{CF}_3$  groups with a possible tilt angle between the  $C_3$  axis and the O-C bond direction. (iii) The difference between the C-O bond lengths,  $\Delta\text{C-O} = \text{C}(\text{sp}^3)\text{-O} - \text{C}(\text{sp}^2)\text{-O}$ , and between the C-F bond lengths,  $\Delta\text{C-F} = \text{C}(\text{sp}^3)\text{-F} - \text{C}(\text{sp}^2)\text{-F}$ , in **1** were set to the calculated values (MP2). An uncertainty of  $\pm 0.005 \text{ \AA}$  was estimated for these differences. (iv) Vibrational ampli-

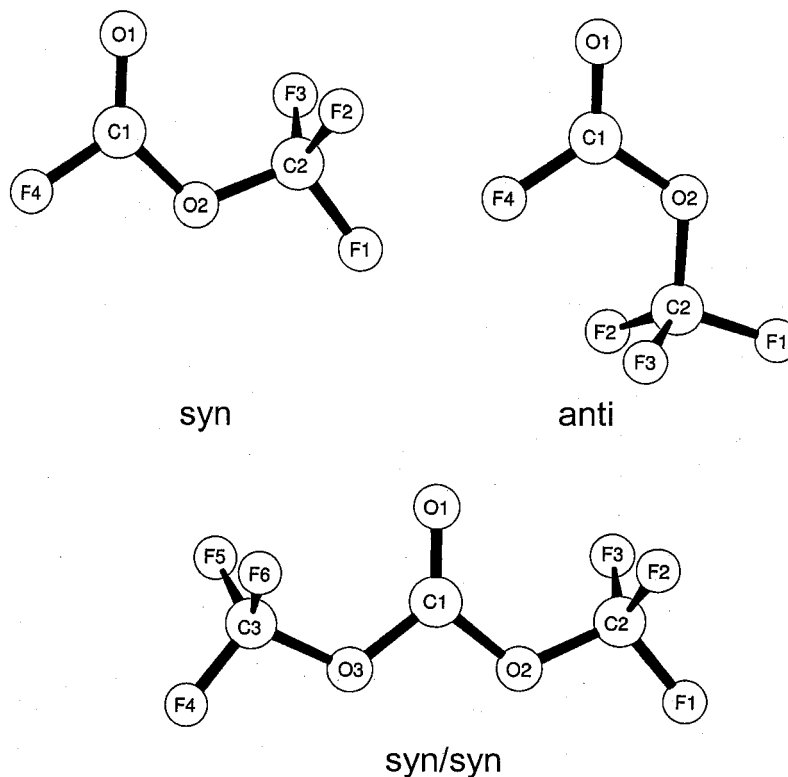


**Figure 7.** Molecular models and numbering of the syn and anti conformers of  $\text{CF}_3\text{OC(O)F}$  and of the syn/syn conformer of  $(\text{CF}_3\text{O})_2\text{CO}$ .

**Table 3.** Experimental and Calculated Geometric Parameters for  $\text{CF}_3\text{OC(O)F}$  (**1**)<sup>a</sup>

	GED <sup>b</sup>		MP2/ 6-311G*	B3LYP/ 6-311G*
C=O	1.188(4)	<i>p</i> 1	1.182	1.177
C—O <sub>mean</sub>	1.364(9)	<i>p</i> 2	1.372	1.375
$\Delta\text{C—O} = \text{C2—O2} - \text{C1—O2}$	0.030[5] <sup>c</sup>		0.030	0.035
C1—O2	1.349(10)		1.357	1.357
C2—O2	1.379(10)		1.387	1.392
C—F <sub>mean</sub>	1.322(3)	<i>p</i> 3	1.322	1.327
$\Delta\text{C—F} = \text{C2—F} - \text{C1—F}$	0.002[5] <sup>c</sup>		0.002	0.004
C1—F	1.321(6)		1.320	1.324
C2—F	1.323(5)		1.322 <sup>d</sup>	1.328 <sup>d</sup>
O1=C1—O2	130.3(16)	<i>p</i> 4	129.0	129.0
O1=C—F4	123.9(20)		125.4	125.1
O2—C1—F4	105.8(12)	<i>p</i> 5	105.6	105.9
C1—O2—C2	117.1(7)	<i>p</i> 6	116.6	118.3
F—C—F	108.9(7)	<i>p</i> 7	109.4	109.3
tilt(CF <sub>3</sub> ) <sup>e</sup>	3.7 <sup>f</sup>		3.7	3.7

<sup>a</sup> Values in angstroms and degrees. For atom numbering see Figure 7. <sup>b</sup> *r*<sub>a</sub> values with 3 $\sigma$  uncertainties. <sup>c</sup> Not refined, varied within the estimated uncertainty in brackets. <sup>d</sup> Mean value. <sup>e</sup> Tilt angle between the C<sub>3</sub> axis and the O—C bond direction, toward the oxygen lone pair. <sup>f</sup> Not refined.

tudes, which either cause large correlations between geometrical parameters or are not well determined in the GED analysis, were constrained to their calculated values. With these assumptions geometric parameters *p*1–*p*7 and vibrational amplitudes *l*1–*l*8 for **1** and *l*1–*l*6 for **2** were refined simultaneously. The following correlation coefficients had values larger than |0.7|: (1) *p*2/*p*3 = -0.94, *p*2/*p*7 = -0.84, *p*3/*p*7 = 0.84, *p*4/*p*6 = -0.73, *p*3/*l*2 = 0.84, and *p*5/*l*3 = 0.70; (2) *p*2/*p*3 = -0.76, *p*3/*p*6 = 0.71, *p*4/*p*7 = 0.86, *p*2/*l*1 = -0.80, *p*4/*l*2 = -0.71, and *p*7/*l*2 = -0.81. The experimental results are listed in Tables 3 and 4 (geometrical parameters) and Tables 5 and 6 (vibrational amplitudes), and molecular models with atom numbering are shown in Figure 7. The fit of the GED intensities of **1** did not

**Table 4.** Experimental and Calculated Geometric Parameters for  $(\text{CF}_3\text{O})_2\text{CO}$  (**2**)<sup>a</sup>

	GED <sup>b</sup>		MP2/ 6-311G*	B3LYP/ 6-311G*
C=O	1.188(9)	<i>p</i> 1	1.187	1.183
C—O <sub>mean</sub>	1.377(5)	<i>p</i> 2	1.373	1.376
$\Delta\text{C—O} = \text{C2—O2} - \text{C1—O2}$	0.024[5] <sup>c</sup>		0.024	0.026
C1—O2	1.365(6)		1.361	1.363
C2—O2	1.389(6)		1.385	1.389
C—F	1.315(3)	<i>p</i> 3	1.323 <sup>d</sup>	1.328 <sup>d</sup>
O1=C1—O2	128.5(15)	<i>p</i> 4	128.1	127.9
O2—C1—O3	103.1(22)		103.8	104.2
C1—O2—C2	116.5(7)	<i>p</i> 5	116.5	118.2
F—C—F	110.2(7)	<i>p</i> 6	109.3	109.3
tilt(CF <sub>3</sub> ) <sup>e</sup>	4.6(21)	<i>p</i> 7	3.7	3.7

<sup>a</sup> Values in angstroms and degrees. For atom numbering see Figure 7. <sup>b</sup> *r*<sub>a</sub> values with 3 $\sigma$  uncertainties. <sup>c</sup> Not refined, varied within the estimated uncertainty in brackets. <sup>d</sup> Mean value. <sup>e</sup> Tilt angle between the C<sub>3</sub> axis and the O—C bond direction, toward the oxygen lone pair.

improve if a contribution of 4% of the anti conformer, as obtained from the matrix IR spectra, was added in the least-squares analysis. Thus, GED intensities in this case are not sensitive toward such small amounts of a second conformer. From the matrix IR spectra of **2** a contribution of less than 1% of the syn/anti rotamer is estimated, and this conformer was not considered in the GED analysis.

## Discussion

In both compounds the synperiplanar orientation of the O—CF<sub>3</sub> groups relative to the C=O double bond is preferred. These conformations are the same as in the parent compounds methyl formate and dimethyl carbonate and are not affected by fluorination. The matrix IR spectra of **1** demonstrated the presence of a small amount of the antiperiplanar conformer, with 4% at room temperature; the contribution of the syn/anti conformer of **2** is estimated to be less than 1%.

**Table 5.** Interatomic Distances and Experimental and Calculated Vibrational Amplitudes for CF<sub>3</sub>OC(O)F (**1**)<sup>a</sup>

	dist	ampl <sup>b</sup> (GED)		ampl (B3LYP)		dist	ampl <sup>b</sup> (GED)		ampl (B3LYP)
C=O	1.19	0.036 <sup>c</sup>		0.036	O1...O2	2.30	0.051 <sup>c</sup>		0.051
C1—F4	1.32	0.042 <sup>c</sup>		0.042	C1...C2	2.33	0.061 <sup>c</sup>		0.061
C2—F1	1.32	0.047(3)	11	0.044	O1...C2	2.76	0.090 <sup>c</sup>		0.090
C1—O2	1.35	0.051(8)	12	0.045	C1...F2	2.78	0.100(10)	14	0.117
C2—O2	1.38	0.051(8)	12	0.048	O1...F2	2.86	0.186 <sup>c</sup>		0.186
O2...F4	2.13	0.056(5)	13	0.055	C1...F1	3.42	0.069(9)	15	0.060
F1...F2	2.15	0.056(5)	13	0.056	C2...F2	3.42	0.069(9)	15	0.061
O2...F1	2.16	0.056(5)	13	0.057	F4...F4	3.95	0.117(14)	16	0.131
O1...F4	2.21	0.050 <sup>c</sup>		0.050	O1...F1	4.05	0.084(24)	17	0.083
O2...F2	2.24	0.059 <sup>c</sup>		0.059	F1...F4	4.28	0.078(18)	18	0.076

<sup>a</sup> Values in angstroms. For atom numbering see Figure 7. <sup>b</sup> 3 $\sigma$  uncertainties. <sup>c</sup> Not refined.

**Table 6.** Interatomic Distances and Experimental and Calculated Vibrational Amplitudes for (CF<sub>3</sub>)<sub>2</sub>CO (**2**)<sup>a</sup>

	dist	ampl <sup>b</sup> (GED)		ampl (B3LYP)		dist	ampl <sup>b</sup> (GED)		ampl (B3LYP)
C=O	1.19	0.036 <sup>c</sup>		0.036	C1...F1	3.41	0.071(12)	14	0.061
C—F	1.32	0.042(3)	11	0.045	O2...C3	3.44	0.071(12)	14	0.061
C1—O2	1.37	0.046 <sup>c</sup>		0.046	O2...F5	3.96	0.132(20)	15	0.134
C2—O2	1.39	0.048 <sup>c</sup>		0.048	O1...F1	4.01	0.096(28)	16	0.083
O2...O3	2.13	0.056(5)	12	0.055	O2...F4	4.24	0.096(28)	16	0.077
O2...F1	2.14	0.058 <sup>c</sup>		0.058	C2...C3	4.65	0.070 <sup>c</sup>		0.070
F1...F2	2.16	0.056(5)	12	0.055	C2...F5	5.01	0.162 <sup>c</sup>		0.162
O2...F2	2.23	0.058 <sup>c</sup>		0.058	F2...F6	5.02	0.278 <sup>c</sup>		0.278
O1...O2	2.30	0.051 <sup>c</sup>		0.051	F2...F5	5.46	0.184 <sup>c</sup>		0.184
C1...C2	2.34	0.061 <sup>c</sup>		0.061	C2...F4	5.57	0.076 <sup>c</sup>		0.076
O1...C2	2.74	0.090 <sup>c</sup>		0.090	F1...F5	6.02	0.173 <sup>c</sup>		0.173
C1...F2	2.77	0.113 <sup>c</sup>		0.113	F1...F4	6.31	0.109 <sup>c</sup>		0.109
O1...F2	2.82	0.169(20)	13	0.176					

<sup>a</sup> Values in angstroms. For atom numbering see Figure 7. <sup>b</sup> 3 $\sigma$  uncertainties. <sup>c</sup> Not refined.

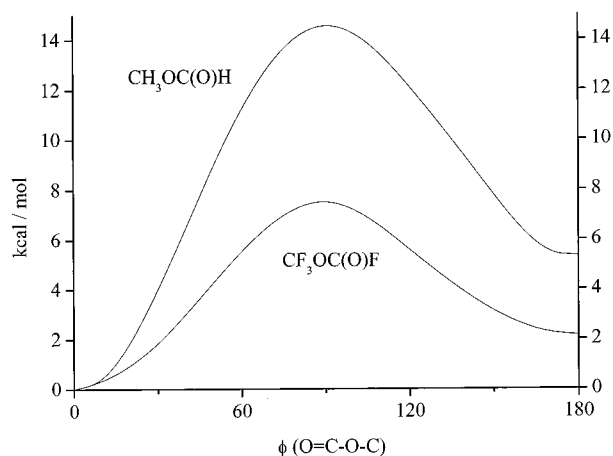
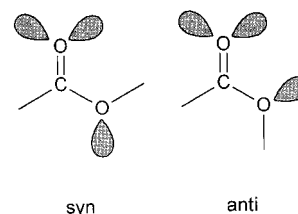
**Figure 8.** Calculated (B3LYP/6-311G\*) potential curves for internal rotation around the C(sp<sup>2</sup>)—O bonds in CH<sub>3</sub>OC(O)H and CF<sub>3</sub>OC(O)F.

Figure 8 shows the calculated potential curves for internal rotation around the C(sp<sup>2</sup>)—O bond for methyl formate and **1**. According to these calculations, the energy difference between syn and anti forms is lowered from 5.3 kcal/mol in the parent species to 2.1 kcal/mol in **1**. Similarly, the barrier to internal rotation decreases from 14.5 to 7.5 kcal/mol upon fluorination. Several explanations have been offered for the experimental observation that in most cases a single bond (O—C(sp<sup>3</sup>) bond in our compounds) eclipses a vicinal double bond rather than a vicinal single bond. Pauling proposed a description of the double bond as a pair of two bent single bonds (banana bonds), and in this picture the single bond staggers the two bent bonds in the synperiplanar structure.<sup>24</sup> Owen and Sheppard<sup>25</sup> pointed out that repulsion between the lone pairs of the two oxygen atoms

**Chart 1****Table 7.** Relevant Orbital Interaction Energies (kcal/mol) between the Oxygen Lone Pairs and the X—C=O Moiety for the Syn and Anti Conformers of CH<sub>3</sub>OC(O)H and CF<sub>3</sub>OC(O)F

	CH <sub>3</sub> OC(O)H		CF <sub>3</sub> OC(O)F	
	syn	anti	syn	anti
$n_{\pi} \rightarrow \pi^*(\text{C}=\text{O})$	-48.2	-44.1	-40.1	-38.4
$n_{\sigma} \rightarrow \sigma^*(\text{C}=\text{O})$	-6.1	-2.1	-7.1	-1.1
$n_{\sigma} \rightarrow \sigma^*(\text{C}(\text{sp}^2)\text{—X})^a$	-1.7	-4.1	-3.4	-7.3
$\Sigma$ interaction energies	-56.0	-50.3	-50.6	-46.8
relative total energies	0.0	5.3	0.0	2.1

<sup>a</sup> X = H or F.

destabilizes the anti conformer and leads to a preference of the syn form (see Chart 1). In formic acid and methyl formate the preference of the syn conformation can be explained by the formation of O...H hydrogen bonds. We have made an attempt to rationalize the preference for the syn conformation of methyl formate and **1** on the basis of a natural bond orbital (NBO) analysis.<sup>26</sup> The stabilizing orbital interactions of the oxygen lone pairs  $n_{\pi}$  and  $n_{\sigma}$  with the X—C=O moiety (X = H or F) are summarized in Table 7 for syn and anti structures of the two compounds. Conjugation between the  $n_{\pi}$  lone pair and the  $\pi^*(\text{C}=\text{O})$  orbital as well as the anomeric interactions between the  $n_{\sigma}$  lone pair and the  $\sigma^*$  orbitals both favor the syn orientation

(24) Pauling, L. *The Nature of the Chemical Bond*; Cornell University Press: Ithaca, NY, 1960.

(25) Owen, N. L.; Sheppard, N. *Proc. Chem. Soc.* **1963**, 264.

(26) Carpenter, J. E.; Weinhold, F. *J. Mol. Struct.: THEOCHEM* **1988**, 169, 41.

in the two compounds. In the case of the anomeric effect it is plausible that the  $n_{\sigma} \rightarrow \sigma^*$  interactions in the syn conformer differ from those in the anti form, since different  $\sigma^*$  orbitals are involved in the two conformations. We have no obvious explanation for the stronger conjugation in the syn than in the anti conformers. The sums of all orbital interactions lead to a preference of the syn form by 5.7 and 3.8 kcal/mol in methyl formate and **1**, respectively. The difference between total energies in methyl formate (5.3 kcal/mol) is very close to the difference between stabilization energies. In the fluorinated derivative the difference between total energies (2.1 kcal/mol) is smaller than that between stabilization energies, indicating higher steric strain in the syn form of this compound. The NBO analysis also allows a qualitative explanation for the decrease of the barrier to internal rotation upon fluorination. The sum of the orbital interaction energies for the perpendicular transition state decreases relative to the syn form by 28.5 kcal/mol in methyl formate, but only by 20.7 kcal/mol in **1**. These decreases, of course, are larger than the calculated barriers of 14.5 and 7.5 kcal/mol, respectively, since steric repulsions are minimized in the perpendicular transition state. The amount by which the stabilization energies decrease in the two compounds parallels the lowering of the barrier to internal rotation upon fluorination.

The effect of fluorination on geometrical parameters is revealed by a comparison with those of methyl formate<sup>1–3</sup> and dimethyl carbonate.<sup>7</sup> Whereas the C1–O2 bonds lengthen slightly by 0.01–0.02 Å upon fluorination, the C2–O2 bonds shorten considerably by 0.04–0.06 Å. The lengthening of the C(sp<sup>2</sup>)–O bonds reflects the decrease of conjugation in the fluorinated compounds (see Table 7). The shortening of the C(sp<sup>3</sup>)–O bonds can be attributed to anomeric interactions between the oxygen lone pairs and the  $\sigma^*(\text{C–F})$  bonds of the CF<sub>3</sub> group and to electrostatic attraction between the negative oxygen and the highly positive carbon atom of the CF<sub>3</sub> group. The increase of the O1=C1–O2 and C1–O2–C2 bond angles by about 2–3° upon fluorination indicates higher steric strain in the fluorinated derivatives.

Whereas the conformational properties of methyl carbonate are not affected by fluorination, those of dimethyltrithio carbonate,  $(\text{CH}_3\text{S})_2\text{C}=\text{S}$ , change appreciably upon fluorination. The GED intensities of the parent species are fitted very well with a single conformer and planar syn/syn structure.<sup>27</sup> A GED analysis for the perfluorinated species,  $(\text{CF}_3\text{S})_2\text{C}=\text{S}$ , resulted in a mixture of 84(12)% syn/syn and 16(12)% syn/anti conformers. The predominant syn/syn form possesses a nonplanar sulfur–carbon skeleton of C<sub>2</sub> symmetry with the S–CF<sub>3</sub> bonds rotated out of the CS<sub>3</sub> plane by 32(4)°.<sup>28</sup>

**Acknowledgment.** This work has been supported by the Deutsche Forschungsgemeinschaft. We thank the Fundación Antorchas (República Argentina), Alexander von Humboldt Stiftung, and DAAD (Deutsche Akademische Austauschdienst, Germany) for financial support and for the DAAD-Fundación Antorchas and Alexander von Humboldt Stiftung-Fundación Antorchas Awards to the German-Argentine cooperation. E.L.V. is indebted to ANPCYT (Argentina) for support. C.O.D.V. also thanks the Consejo Nacional de Investigaciones Científicas y Técnicas (CONICET), ANPCYT (PICT 122) (Argentina), and Comisión de Investigaciones Científicas de la Provincia de Buenos Aires (CIC), República Argentina, for financial support. He is indebted to the Facultad de Ciencias Exactas, Universidad Nacional de La Plata, República Argentina, for financial support and to the Fundación Antorchas for the National Award to the Argentinean cooperation.

**Supporting Information Available:** Tables of calculated (B3LYP/6-31G\*) vibrational frequencies and IR intensities for  $\text{CF}_3\text{OC}(\text{O})\text{F}$  (Table S1) and  $(\text{CF}_3\text{O})_2\text{CO}$  (Table S2). This material is available free of charge via the Internet at <http://pubs.acs.org>.

IC010066A

(27) Almenningen, A.; Fernholt, L.; Seip, H. M.; Henriksen, L. *Acta Chem. Scand.* **1974**, A28, 1037.

(28) Hermann, A.; Ulic, S. E.; Della Vedova, C. O.; Lieb, M.; Mack, H.-G.; Oberhammer, H. *J. Mol. Struct.* **2001**, 556, 217.